

# Thermoelectric Converter for Loop Heat Pipe Temperature Control: Experience and Lessons Learned

Jentung Ku<sup>1</sup> and Laura Ottenstein<sup>2</sup>  
NASA Goddard Space flight Center, Greenbelt, Maryland, 20771, USA

This paper describes the theoretical background and implementation methodology of using a thermoelectric converter (TEC) for operating temperature control of a loop heat pipe (LHP). In particular, experimental results from ambient and thermal vacuum tests of an LHP are presented for illustrations. The most commonly used state-of-the-art method to control the LHP operating temperature is to cold bias its compensation chamber (CC) and use an electrical heater to maintain the CC at the desired set point temperature. Although effective, this approach has its shortcomings in that the electrical heater can only provide heating to the CC, and the required power can be large under certain conditions. An alternative method is to use a TEC, which is capable of providing both heating and cooling to the CC. In this method, one side of the TEC is attached to the CC, and the other side is connected to the evaporator via a thermal strap. Using a bipolar power supply and a control algorithm, a TEC can function as a heater or a cooler, depending on the direction of the current flow. Extensive ground tests of several LHPs have demonstrated that a TEC can provide very tight temperature control for the CC. It also offers several additional advantages: (1) The LHP can operate at temperatures below its natural operating temperature at low heat loads; (2) The required heater power for a TEC is much less than that for an electrical heater; and (3) It enhances the LHP start-up success. Although the concept of using a TEC for LHP temperature control is simple, there are many factors to be considered in its implementation for space applications because the TEC is susceptible to the shear stress and yet has to sustain the dynamic load under the spacecraft launch environment. The added features that help the TEC to withstand the dynamic load will inevitably affect the TEC thermal performance. Some experiences and lessons learned are addressed in this paper.

## Nomenclature

$C_p$	=	specific heat of working fluid
$G_{strap}$	=	thermal conductance across thermal strap (including interface conductance at both ends)
$G_{E,CC}$	=	thermal conductance between evaporator and compensation chamber
$m$	=	mass flow rate
$Q_{cc}$	=	compensation chamber power
$Q_E$	=	heat load applied to evaporator
$Q_{High}$	=	highest evaporator power below which CC can be controlled at $T_{set}$ through heating
$Q_{leak}$	=	heat leak from evaporator to compensation chamber

---

<sup>1</sup> Laboratory Manager, Thermal Engineering Branch, Goddard Space Flight Center, Greenbelt, Maryland, USA, AIAA Senior Member

<sup>2</sup> Aerospace Engineer, Thermal Engineering Branch, Goddard Space Flight Center, Greenbelt, Maryland, USA

- $Q_{Low}$  = lowest evaporator power above which CC can be controlled at  $T_{set}$  through heating  
 $Q_{strap}$  = heat flow through the thermal strap  
 $Q_{sub}$  = amount of liquid subcooling  
 $Q_{TEC,app}$  = heat applied to thermoelectric converter  
 $Q_{TEC,H}$  = heat delivered to the hot side of thermoelectric converter  
 $Q_{TEC,L}$  = heat absorbed by thermoelectric converter at the cold side  
 $T_{CC}$  = temperature of compensation chamber  
 $T_E$  = temperature of evaporator  
 $T_{in}$  = temperature at the inlet of compensation chamber  
 $T_{SET}$  = compensation chamber set point temperature  
 $T_{TEC,H}$  = temperature at the hot side of thermoelectric converter  
 $T_{TEC,L}$  = temperature at the cold side of thermoelectric converter  
 $\lambda$  = latent heat of vaporization of the working fluid  
 $\Delta T$  = temperature difference

## I. Introduction

A LOOP heat pipe (LHP) is a very robust and versatile heat transfer device which can transport large heat loads over long distances with small temperature differences<sup>1,2</sup>. LHPs are being used on several commercial communications satellites and NASA's ICESat, SWIFT, AURA, GOES-N and GOES-R spacecraft<sup>3-11</sup>. The LHP operating temperature is governed by the saturation temperature of its compensation chamber (CC); the latter is a function of the heat leak from the evaporator to the CC, the amount of subcooling carried by the liquid returning to the CC, and the amount of heat exchanged between the CC and ambient. For a well-insulated CC, the heat exchange between the CC and ambient can be ignored, and the heat leak is balanced by the liquid subcooling as shown in Figure 1. Thus,

$$Q_{leak} - Q_{sub} = 0 \quad (1)$$

$$Q_{leak} = G_{E,CC} (T_E - T_{CC}) \quad (2)$$

$$Q_{sub} = m C_p (T_{CC} - T_{in}) \quad (3)$$

$$m = Q_E / \lambda \quad (4)$$

The heat leak is usually a few percent of the heat load applied to the evaporator. The amount of subcooling is a function of the condenser sink temperature, ambient temperature and evaporator heat load. When the ambient temperature is higher than the condenser sink temperature, the CC temperature as a function of the evaporator heat load yields a well-known V-shaped curve as shown in Fig. 2.

Many spacecraft applications require a narrow temperature range, but also constrain power usage. The LHP operating temperature can be controlled at a fixed set point required by the instrument (e.g.  $T_{SET}$  as shown in Fig. 3) by adding heat to or removing heat from the CC. As shown in Fig. 4, the energy balance becomes:

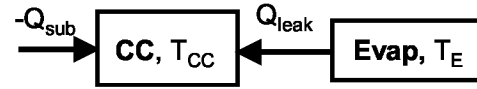


Figure 1. Energy Balance for Insulated CC

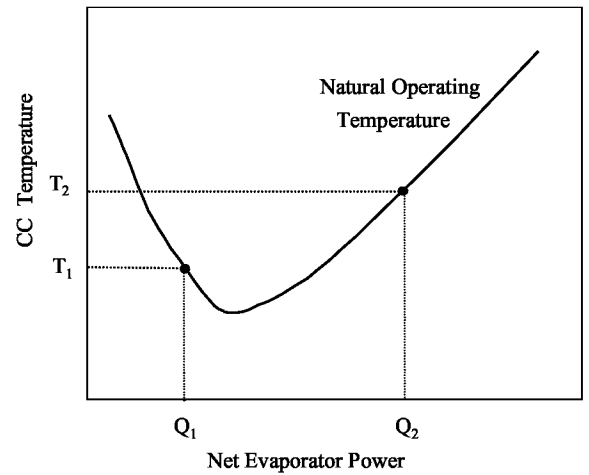


Figure 2. LHP Natural Operating Temperature

$$Q_{leak} - Q_{sub} + Q_{CC} = 0 \quad (5)$$

Thus,

$$Q_{CC} = Q_{sub} - Q_{leak} \quad (6)$$

A positive  $Q_{CC}$  denotes the heat to be added to the CC whereas a negative  $Q_{CC}$  denotes the heat to be removed. In Fig. 3,  $Q_{CC}$  is positive and the CC requires heating for evaporator heat loads between  $Q_{Low}$  and  $Q_{High}$ . For evaporator heat loads smaller than  $Q_{Low}$ ,  $Q_{CC}$  is negative and the CC requires cooling. For evaporator heat load greater than  $Q_{High}$ , the LHP's natural operating temperature is greater than  $T_{SET}$ , and the only practical method to maintain the CC temperature at  $T_{SET}$  is to increase the condenser heat dissipating capacity, i.e. to increase the radiator area.

The most commonly used method to control the CC saturation temperature is to cold bias the CC and use an electrical heater. This method has been proven to be effective, but it also has its shortcomings. First, the electrical heater can only provide heating to the CC, i.e. the set point temperature  $T_{SET}$  can only be maintained for the evaporator heat load between  $Q_{Low}$  and  $Q_{High}$ , as illustrated in Fig. 3. Second, the required CC control heater power can be very large when the condenser sink is very cold.

Several methods have been used to reduce the control heater power requirement, including using aluminum coupling blocks installed between the vapor line and liquid line<sup>3-7</sup>, using a variable conductance heat pipe that connects the evaporator and the liquid line<sup>8-11</sup>, using a vapor by-pass valve to divert part of the vapor from the vapor line to the liquid line<sup>12-16</sup>, and using a heat exchanger between the vapor line and liquid line and a separate subcooler<sup>17</sup>. As summarized in References 18 and 19, these methods are generally effective in reducing the CC control heater power. Nevertheless, the lack of an ability for actively cooling the CC remains.

Studies have been conducted to investigate the feasibility of using a thermoelectric converter (TEC) to provide cooling as well as heating to the CC. In this approach, one side of the TEC is attached to the CC, and the other side is connected to the evaporator via a thermal strap. Using a bipolar power supply and a control algorithm, the TEC automatically changes its mode of operation between heating and cooling the CC. This paper summarizes the results of such studies, including the theoretical background, implementation methodology, and some lessons learned. For illustration purposes, experimental results from testing of an LHP are discussed.

## II. TEC for LHP Temperature Control

A TEC operates based on the Peltier effect, which states that when an electric current flows through two dissimilar conductors, the junction of the two conductors will either absorb or release heat depending on the direction of the current flow. Details of the operating principles, construction, and performance characteristics of TECs can be found in the literature<sup>20</sup> and on TEC vendors' web sites. The amount of heat that a TEC can pump is a function of the TEC design, the power that drives the TEC, the temperature at the TEC hot side, and the temperature difference between TEC's hot and cold sides. There are different ways to present the performance characteristics of a TEC. One of the methods is depicted in Fig. 5, which shows performance curves of the Marlow Industries model DT3-6 TEC at a hot side temperature of 300K. The bottom chart displays the relationship between the voltage applied to the TEC and the electric current that will flow through the TEC. The top chart shows the amount of heat pumped by the TEC and the temperature differential between the hot and cold sides of the TEC for the given voltage and current. The upper curve on the bottom chart ( $Q = 0$ ) indicates an extreme condition under which the TEC pumps no heat, and correspondingly the uppermost curve on the top chart (heat load = 0) shows the maximum  $\Delta T$

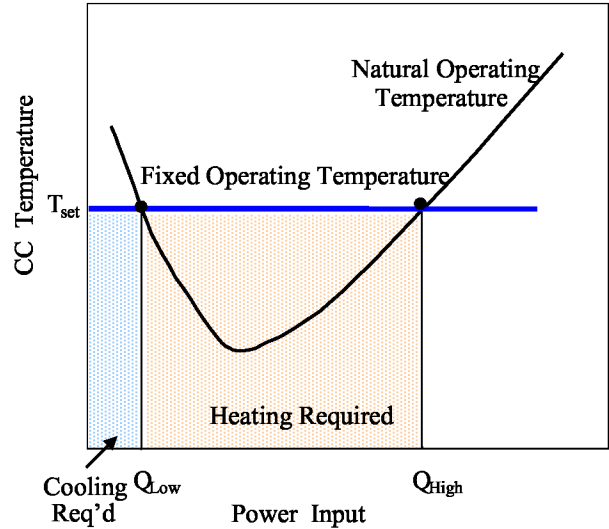


Figure 3. LHP Operating Temperature Control

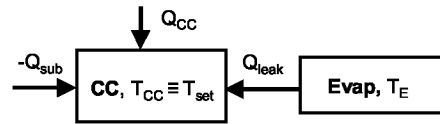


Figure 4. Energy Balance for CC

that can be developed across the TEC. The lower curve on the bottom chart ( $\Delta T = 0$ ) shows another extreme condition where the two sides of the TEC are kept at the same temperature, and the intersection of the heat load curves with the horizontal line of  $\Delta T = 0$  on the top chart indicates the maximum heat that the TEC can pump. In most practical applications, the voltage-current curve will fall between the two extreme conditions, and some heat will flow through the TEC with a temperature difference built up between the hot and cold sides of the TEC.

When the direction of the current is reversed, the hot side and the cold side of the TEC will switch, and the direction of the heat flow will also reverse. In other words, the TEC can switch its mode of operation from heating an object to cooling it, or vice versa. This is what makes a single TEC capable of switching its operation between heating and cooling the same object as required.

When a TEC is used to control the CC set point temperature in an LHP, one side of the TEC can be attached to a copper saddle which is mounted to the CC, and the other side can be connected to the evaporator via a thermal strap as shown in Figure 6. Using a bipolar power supply and a control algorithm, the TEC will automatically switch its mode of operation between heating and cooling to maintain the CC at the desired temperature. One can even use a proportional-integral-derivative (PID) temperature control scheme so that the applied voltage can be varied (up to the allowable upper limit for the given TEC). Note that the hot side of the TEC must have a proper heat sink for heat dissipation. Otherwise, the hot side will get hotter and hotter. When the temperature difference between the hot side and cold side exceeds the  $\Delta T$  value corresponding to heat load = 0 showing on the top chart of Fig. 5, the TEC will cease to pump heat altogether. Thus, the thermal strap must be properly designed to provide sufficient thermal conductance so that the TEC will not reach the 0W heat load limit.

Fig. 6 shows the heat flow where the TEC is heating the CC. As a current (power) is applied to the TEC, the side that is attached to the CC becomes the hot side and is maintained at the CC set point temperature. The other side, which is attached to the thermal strap, becomes cold. Because the evaporator is warmer than the CC, a temperature difference is therefore created across the thermal strap. Consequently, heat will flow from the evaporator toward the CC. This heat plus the heat that is applied to the TEC will be delivered to the CC for heating:

$$Q_{cc} = Q_{TEC,H} = Q_{TEC,L} + Q_{TEC,app} \quad (7)$$

$$Q_{TEC,L} = Q_{Strap} = G_{strap} (T_E - T_{TEC,L}) \quad (8)$$

$$Q_{TEC,app} \leq Q_{CC} \quad (9)$$

$Q_{TEC, app}$  is the external power applied to the TEC.  $Q_{cc}$  is the power required to maintain the CC at its set point temperature. An electric heater supplying a power of  $Q_{cc}$  will satisfy this requirement. The power savings when a TEC is used is therefore equal to  $Q_{Strap}$ , the heat flowing through the thermal strap.

When the TEC is cooling the CC as is shown in Fig. 7, the power applied to the TEC plus the heat that is pumped from the CC is delivered to the hot side of the TEC. The heat is then transferred via the thermal strap to the evaporator, and is ultimately dissipated to the condenser if the LHP is operational. In addition to Eq. (7), one can write the following equations:

Hot Side Temperature: 27°C

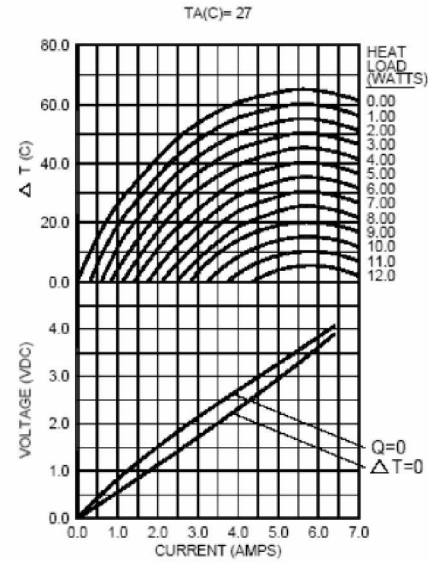


**Figure 5. Performance Curves for Marlow Industries Model DT3-6 TEC at a Hot Side Temperature of 300K**

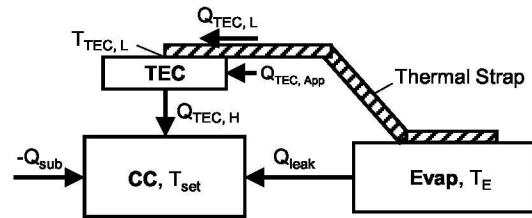


**Figure 6. Schematic of TEC Heating CC**

$$Q_{CC} = Q_{TEC,L} \quad (10)$$

$$Q_{TEC,H} = Q_{Strap} = G_{strap}(T_{TEC,H} - T_E) \quad (11)$$

When the TEC is heating the CC, the cold side will reach an equilibrium temperature,  $T_{TEC,L}$ , which simultaneously satisfies the following conditions: 1) The TEC will pump a heat load of  $Q_{load}$  which is bound by the TEC performance curves shown in Fig. 5 based on the power (voltage and the corresponding current) applied to the TEC and the  $\Delta T$  across the TEC; 2)  $Q_{load}$  is equal to  $Q_{TEC,L}$ ; 3)  $Q_{TEC,L}$  is the heat transmitted from the evaporator through the thermal strap, and must be governed by Eq. (8); and 4) A heat load of  $Q_{TEC,H}$ , which is the sum of  $Q_{TEC,L}$  and  $Q_{TEC,app}$ , is delivered to the hot side of the TEC, and is ultimately dissipated to the CC.

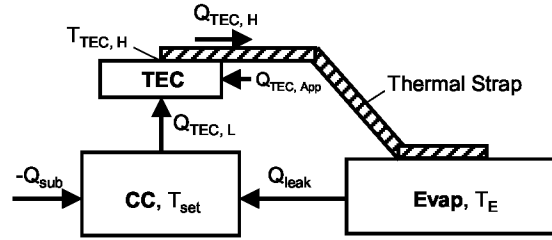


Figure 7. Schematic of TEC Cooling CC

When the TEC is cooling the CC, the TEC hot side will reach an equilibrium temperature,  $T_{TEC,H}$ , which simultaneously satisfies the following conditions: 1) The TEC will pump a heat load of  $Q_{load}$ , which is bound by the TEC performance curves shown in Fig. 5 based on the power (voltage and the corresponding current) applied to the TEC and the  $\Delta T$  across the TEC. 2)  $Q_{load}$  is equal to  $Q_{TEC,L}$ , the heat pumped from the CC, 3) A heat load of  $Q_{TEC,H}$ , which is the sum of  $Q_{TEC,L}$  and  $Q_{TEC,app}$ , is delivered to the hot side of the TEC; and 4)  $Q_{TEC,H}$ , which is the heat transmitted to the evaporator through the thermal strap, is governed by Eq. (11).

TECs have been used to control the operating temperature of an LHP with a single evaporator<sup>21</sup>, and three LHPs with two evaporators and two condensers<sup>22-28</sup>. In all ground tests, the TECs were able to provide tight temperature control for the LHPs, and the control heater power was much less than that for the electrical heater. In addition, the LHPs could be started successfully using TEC alone without applying a heat load to the evaporator. In the following discussions, experimental results from testing a miniature LHP (MLHP) with two evaporators and two condensers used in the Thermal Loop experiment under NASA's New Millennium Program Space Technology 8 (ST 8) Project will be used to illustrate the LHP/TEC operation.

### III. MLHP for ST 8 Thermal Loop Experiment

The MLHP used in the ST 8 Thermal Loop experiment consisted of two parallel evaporators, two parallel condensers, a common vapor transport line and a common liquid return line. A schematic of the design concept is shown in Fig. 8. Fig. 9 shows a picture of the actual hardware of the MLHP Breadboard test article and Table 1 summarizes major design parameters. An aluminum block with a 400-gram mass was attached to each evaporator to simulate the instrument. The two parallel condensers were sandwiched between two aluminum plates. A flow regulator consisting of capillary wicks was installed at the downstream of the two condensers. The vapor and liquid lines were coiled to yield the required transport length in the given space and to provide flexibility for different test configurations. Several aluminum coupling blocks (20 mm by 20mm by 6mm each) were used to connect the vapor line and liquid line to serve as heat exchangers. A TEC made by Marlow Industries with a model number DT3-6 was installed on each CC through an aluminum saddle. The other side of the

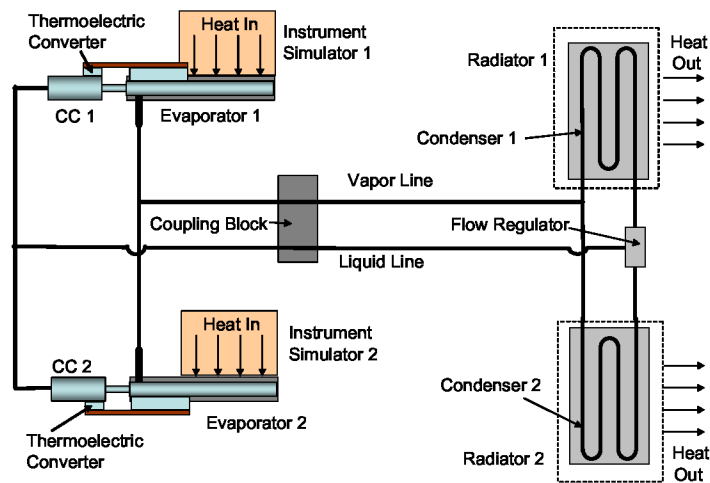


Figure 8. Thermal Loop Experiment Concept

Several aluminum coupling blocks (20 mm by 20mm by 6mm each) were used to connect the vapor line and liquid line to serve as heat exchangers. A TEC made by Marlow Industries with a model number DT3-6 was installed on each CC through an aluminum saddle. The other side of the



TEC was connected to the evaporator via a copper strap. A close-up view of the evaporator/CC section is depicted in Fig. 10.

A cartridge heater capable of delivering 1W to 200W was inserted into each aluminum thermal mass. The applied power was obtained from the multiplication of the measured voltage and measured current. Each TEC was controlled by a bi-polar power supply. Changing the polarity of the applied voltage changed the direction of the current flow and the mode of the TEC operation between heating the CC and cooling the CC. The MLHP Breadboard was tested in the laboratory and the thermal vacuum chamber. For ambient tests in the laboratory, each condenser was attached to a cold plate, and each cold plate was convectively cooled by a chiller. In the thermal vacuum test, each condenser/radiator was cooled by a cryopanel through radiation on one side (the down-facing side). Two copper cryopanel were used as radiator sinks, one for each radiator. Several electric heaters were placed on the top-facing side of the radiators so that the temperatures of the two radiators could be varied independently.

Table 1. MLHP Breadboard Major Design Parameters

Component	Material	Value
Evaporators (2)	Aluminum 6061	9 mm O.D. x 52 mm L
Primary Wicks (2)	Titanium	6.35 mm O.D. x 3.2mm I.D Porosity: 0.35 Pore radius 1.39 $\mu\text{m}$ (E1), 1.47 $\mu\text{m}$ (E2) Permeability: $0.11 \times 10^{-13}\text{m}^2$ (E1), $0.09 \times 10^{-13}\text{m}^2$ (E2)
Secondary Wicks (2)	Stainless Steel	Porosity: 0.67 Pore radius: 68.7 $\mu\text{m}$ Permeability: $83 \times 10^{-13}\text{m}^2$
Bayonet Tubes (2)	SS 304L	1.1 mm O.D. x 0.79 mm I.D.
CC (2)	SS 304L	22.2 mm O.D. x 21.2 mm I.D. x 72.4 mm L
Vapor Line	SS 304L	2.38 mm O.D. x 1.37 mm I.D. x 914 mm L
Liquid Line	SS 304L	1.59 mm O.D. x 1.08 mm I.D. x 914 mm L
Condensers (2)	SS 304L	2.38 mm O.D. x 1.37 mm I.D. x 2540 mm L
Flow Regulator	SS	Pore radius: 10.1 $\mu\text{m}$ Permeability: $3.1 \times 10^{-13}\text{m}^2$
Working Fluid	Ammonia	29.3 grams
Total LHP Mass		316.6 grams

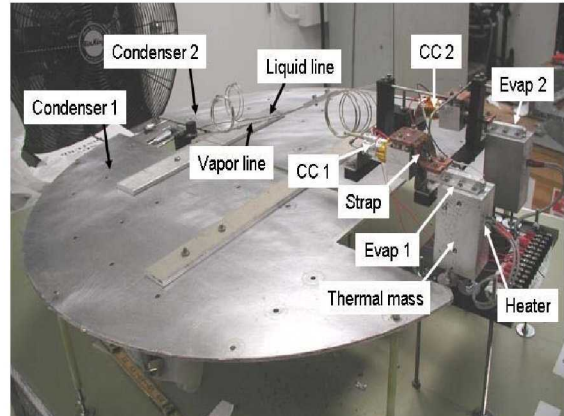


Figure 9. Picture of the MLHP Breadboard

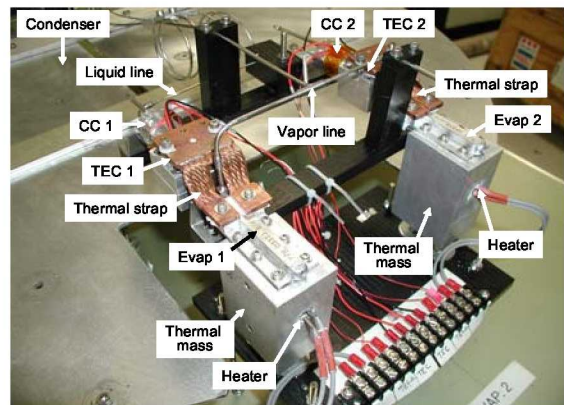
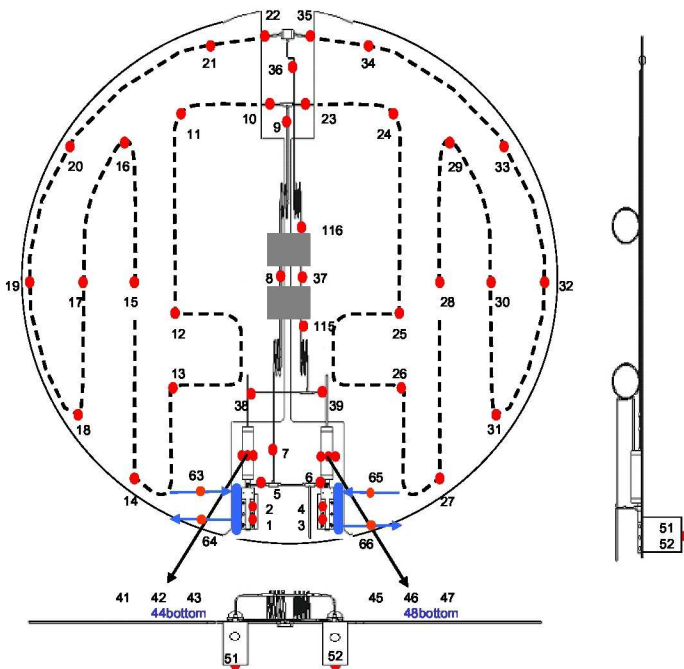


Figure 10. Close-up View of the Evaporator and CC

More than 60 type T thermocouples were used to monitor the MLHP temperatures, as shown in Fig. 11. A data acquisition system consisting of a data logger, a personal computer, and two screen monitors was used to collect and store temperature and power data every second. Labview software was used for the command and control of the test conditions. In particular, a PID control scheme with a specified maximum allowable voltage to be applied to the TEC was used to control the CC set point temperature.

To investigate the effect of the thermal conductance of the strap on the TEC operation, two types of copper thermal strap design were used in the test as shown in Figures 12 and 13, respectively. The first type of strap has a thermal conductance of 0.22W/K, and the second 0.5W/K. These thermal conductance values were obtained from thermal vacuum testing of both types of straps. Two straps of each type were used, one for each CC/evaporator pair. In addition, various numbers of aluminum coupling blocks were used: 0, 2, 3 and 4 blocks.



**Figure 11. Thermocouple Locations**



**Figure 12. Type 1 Thermal Strap**



**Figure 13. Type 2 Thermal Strap**

#### IV. TEC/MLHP Breadboard Performance

The TEC attached to the CC serves three purposes: 1) to provide active cooling to the CC to maintain the CC set point temperature; 2) to replace traditional electric heaters to heat the CC and maintain the CC set point temperature; and 3) to reduce the control heater power when heating the CC. Thus, the objectives of the TEC performance tests are to demonstrate that: 1) The TEC can maintain a stable CC set point temperature during steady state and transient operations of the LHP; 2) Through TEC's active cooling of the CC, the LHP can operate at temperatures below its natural operating temperature at low evaporator heat loads; 3) Through its active cooling of the CC, the TEC could enhance the LHP start-up success even under the worst case initial condition; and 4) The TEC control heater power is lower than that of an electrical heater under the same test condition. Extensive tests have been conducted on several LHPs using TECs and all of these objectives were met. Some experimental results of the TEC/MLHP Breadboard tests are highlighted below. In all plots and descriptions, the following abbreviations are used: E1 – evaporator 1, E2 - evaporator 2, CC1 – compensation chamber 1, CC2 – compensation chamber 2, C1 – condenser 1, C2 – condenser 2.

Both Type 1 and Type 2 thermal straps were used and both could allow the TEC to maintain the CC set point under all test conditions. Using Type 2 thermal strap resulted in a smaller TEC control heater power when compared to Type 1 thermal strap because of a higher thermal conductance possessed by the Type 2 thermal strap. Fig. 14 shows the required TEC power as a function of the evaporator heat load when both CCs were kept at 303K and both condenser sinks were kept at 273K, whereas Fig. 15 shows the results when both CCs were kept at 313K and both condenser sinks were kept at 253K. Results included tests with 0 and 2 coupling blocks connecting the vapor and liquid lines. For a given evaporator heat load, the CC and evaporator temperature were fixed, so the amount of heated required by the CC to maintain a constant set point temperature was also fixed. A higher strap thermal conductance allowed heat to be transmitted more easily from the evaporator to the TEC cold side. This also reduced the  $\Delta T$  across the TEC hot and cold sides, and made the TEC work more efficiently. Consequently, the required TEC power was reduced according to Fig. 5. The aluminum couple blocks allowed the liquid line to be pre-heated by exchanging heat with the vapor line, thereby reducing the required heater power for TECs.

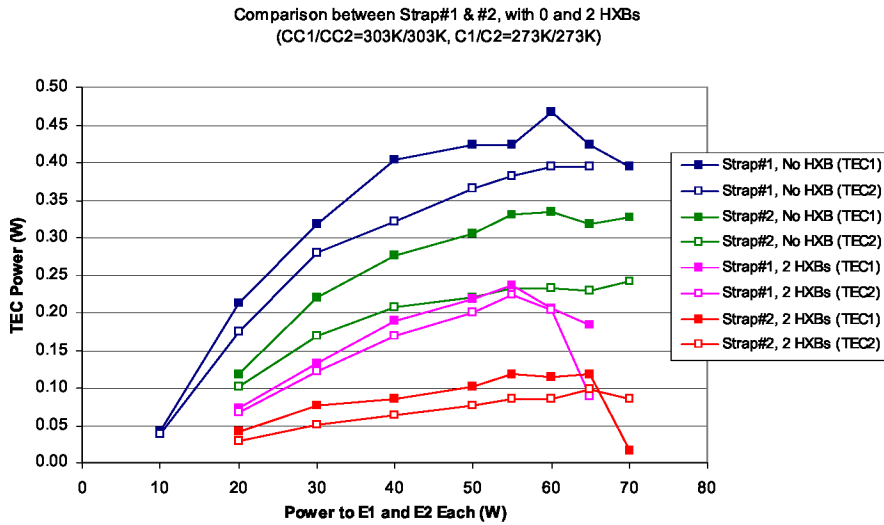


**Figure 14. Required TEC Power Using Different Thermal Straps (CC at 303K)**

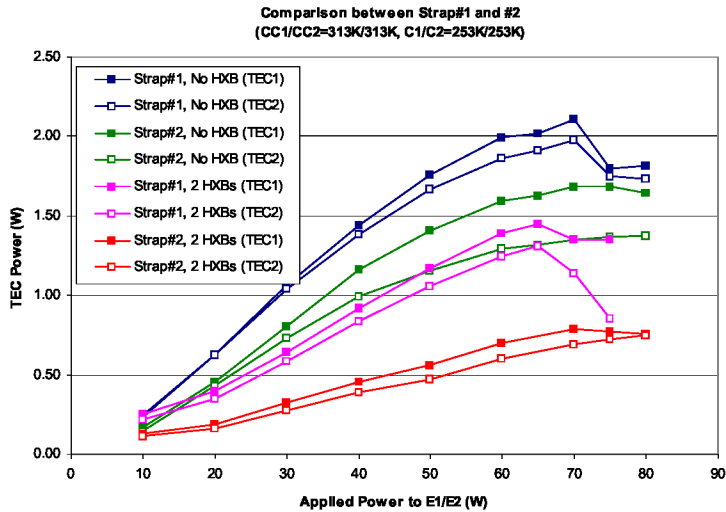


**Figure 15. Required TEC power Using Different Thermal Straps (CC at 313K)**

Note that the MLHP Breadboard had a heat transport limit of 60W/60W to E1/E2 at 303K and 65W/65W at 313K. When the heat transport limit was exceeded, vapor penetrated the primary wick and led to a higher heat leak from the evaporator to the CC, resulting in a smaller TEC control heater power requirement.

Figure 16 shows the loop temperatures in an ambient test where the heat load to E1/E2 varied between 75W/0W and 0W/75W while the C1 sink temperature was kept at 273K and C2 sink temperature varied between 263K and 293K. Type 2 thermal straps were used and no coupling block was attached. The TECs were able to control the loop operating temperature within  $\pm 0.5K$  of the desired 303K set point temperature at all times regardless of whether CC1, CC2, or both were being controlled, and regardless of changes of the evaporator heat load distribution and the condenser sink temperature. The required TEC power to maintain each CC temperature was less than 2W, which was typical for all tests.



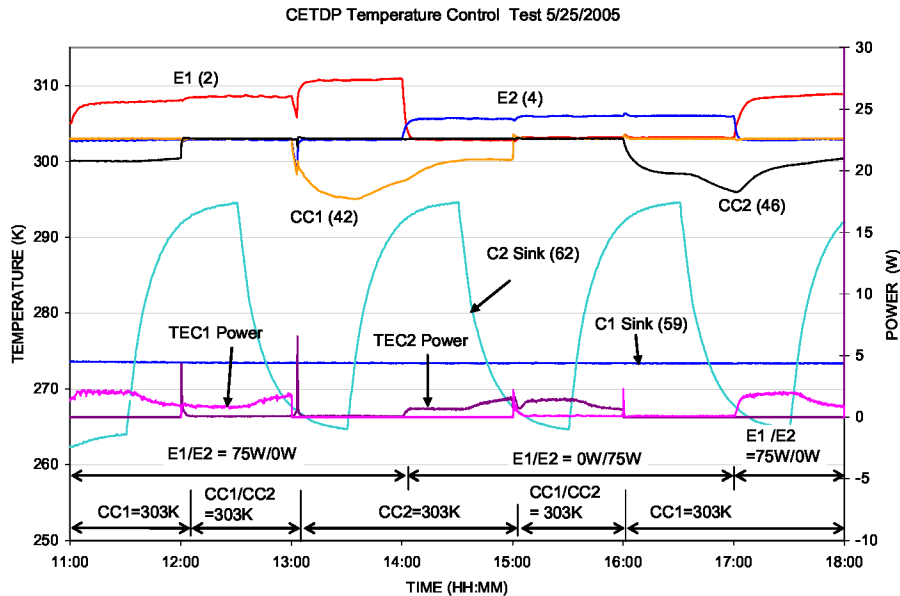


**Figure 16. Saturation Temperature Control Using TECs**

Fig. 17 depicts the loop temperatures during a CC set point change test in a thermal vacuum chamber. A heat load of 10W/10W was applied to E1/E2, and the cryopanel were kept at 223K/223K. The CC1/CC2 temperatures were changed in steps: 293K/293K, 288K/288K, 283K/283K, 278K/278K, and 273K/273K using both TECs. As the CC1/CC2 set points were changed, temperatures of E2 and vapor line followed the change. For clarity, the E1 temperature is not shown in the figure, but it was almost the same as the E2 temperature. After the loop had operated at 273K for about 30 minutes, both TECs were turned off, and the loop gradually approached its natural operating temperature around 282K. Both evaporators and the vapor line followed the change. This test clearly illustrated that, using TECs, the loop could operate at temperatures below its natural operating temperature.

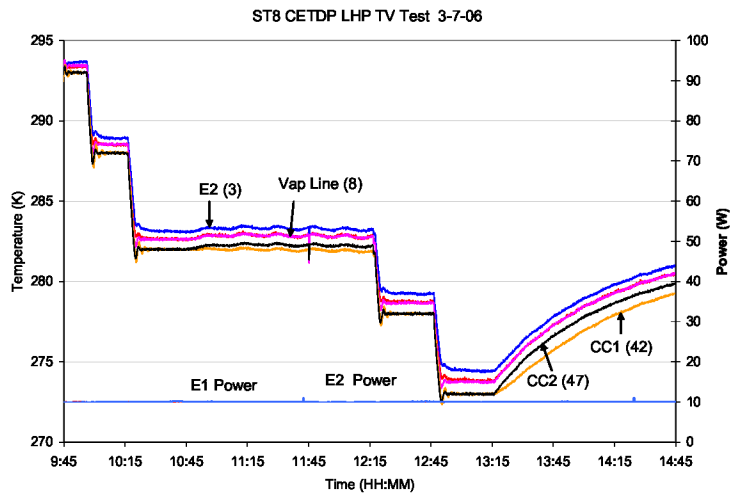


**Figure 17. CC Set Point Change Test**

Start-up at low heat loads could be problematic for LHPs, especially at the so-called “worst-case initial condition” where the evaporator grooves are completely filled with liquid and the evaporator core has two-phase fluid<sup>2, 29</sup>. The problem arises because a superheat is required to initiate boiling in the grooves, but a large heat leak from the evaporator to the CC through the two-phase core continues to raise the CC temperature, rendering the required superheat unachievable as shown in Fig. 18(a). The ability of a TEC to provide cooling will keep the CC temperature constant so that the required superheat can eventually be reached, as shown in Fig. 18 (b). Successful start-up can also be accomplished by lowering the CC temperature using the TEC instead of raising the evaporator temperature as illustrated in Fig. 18(c).

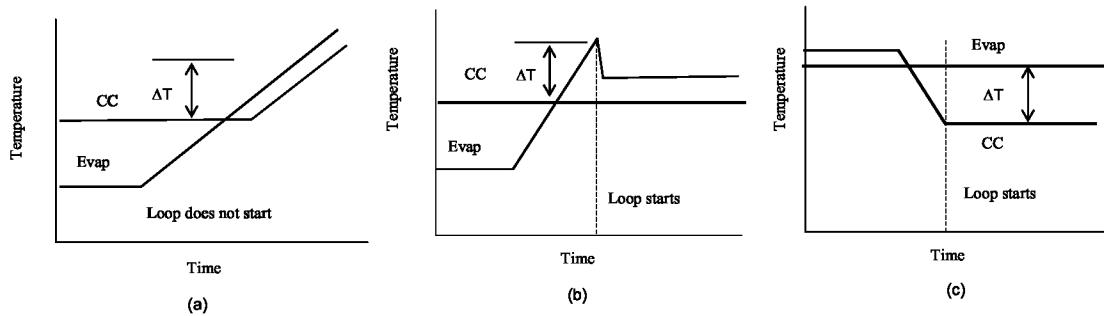


Figure 18. Some Start-up Scenarios

More than 200 start-up tests were performed on the MLHP Breadboard in ambient and thermal vacuum chamber tests. All start-up tests were successful, including some tests where the worst-case initial conditions were purposely created<sup>30</sup>. In addition, several tests were conducted to demonstrate the feasibility of using the TEC to start the loop by lowering the CC temperature as illustrated in Fig. 18(c). Fig. 19 shows that, in thermal vacuum testing, the CC temperatures were lowered from 293K to 258K in steps with 5K increments using TECs. The cryopanel was set at 173K/173K throughout the test. The loop actually started when the CC temperatures were lowered to 288K. The loop was operational because temperatures of the evaporators, transport lines, and thermal masses all moved in tandem with the change of the CC temperatures. The heat input to the evaporators came from several sources, including parasitics, power that was applied to the TECs, and the heat that was pumped out of the CCs. Once the loop was running, an additional heat source came from the release of the sensible heat by the thermal masses. Because the loop had already started, when a heat load of 10W/10W was applied to E1/E2, the event was simply a change of the heat load so far as the loop was concerned.

Tests were conducted to compare the control heater power requirements for the TEC and electrical heater as a function of the evaporator heat load with two coupling blocks and without any block. Tests were performed using TECs alone first, and then using electric heaters alone. Fig. 20 shows the results of tests where both CCs were maintained at 313K and both condenser sinks at 253K. It can be seen that adding

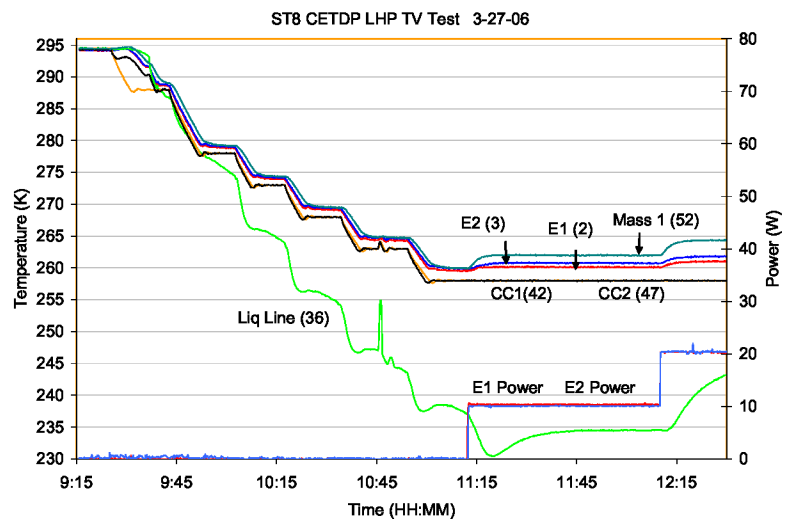


Figure 19. CC Set Point Change and Loop Operation at 258K

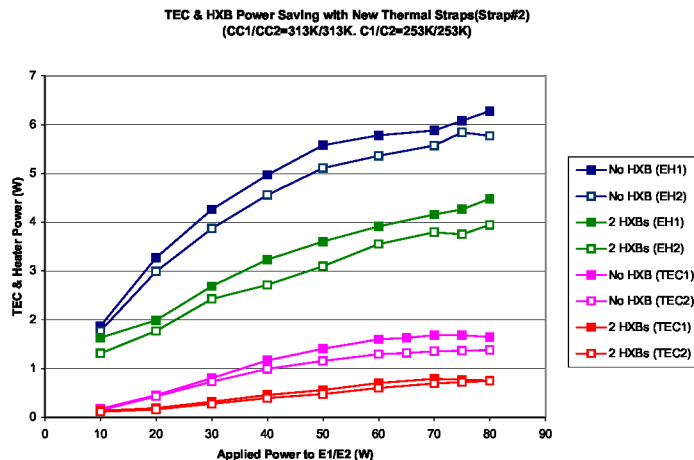


Figure 20 Power Required to Control CC Saturation Temperature at 313K

coupling blocks reduced the required control heater power regardless of whether TECs or electrical heaters were used. Using TECs, however, reduced the control heater power by more than 60 percent when compared to using electric heaters. Similar results were obtained in tests where the CCs were kept at 303K and the condenser sinks were at 273K.

## V. Some Lessons Learned

The voltage and current relationship shown in Fig. 5 is important in implementing the TEC for CC set point temperature control. It should be noted that the voltage shown is the voltage across the TEC terminals. In the early stage of the MLHP Breadboard test program, it was found that the voltage and current measured at the power supply did not match the voltage-current relationship shown in Fig. 5. After some investigations, it was realized that the TEC is a high current, low voltage device and that the voltage drops in the transmission lines between the power supply and the TEC cannot be ignored. Measurements of the voltage drops across the TECs were then made, and were plotted against the voltage drops at the power supply, as shown in Figure 21. This correlation was used in subsequent control scheme for the TEC heater power. The measured voltage drops across the TECs matched very well the voltage-current relationship illustrated in Fig. 5. The lesson learned is that the voltage drops in the transmission lines between the power supply and the TEC must be accounted for if a direct measurement of the voltage drop across the TEC itself is impractical or impossible.

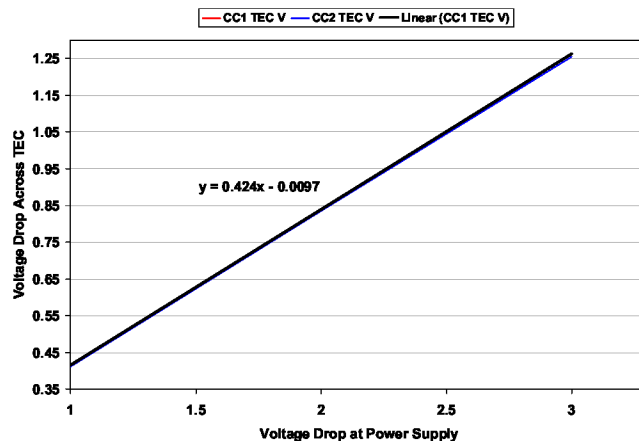


Figure 21. Voltage Drops Across TEC and Power Supply

Although the concept of using a TEC for LHP temperature control is simple, there are many factors to be considered in its implementation for space applications because the TEC is susceptible to the shear stress and yet has to sustain the dynamic load under the spacecraft launch environment. The added features that help the TEC to withstand the dynamic load will inevitably affect the TEC thermal performance. Specifically, the following factors will impact the TEC performance: (1) the thermal conductance of the strap connecting the TEC and the evaporator; (2) the back conduction through the TEC itself and through its mounting saddle; and (3) the back conduction through a redundant TEC.

The effect of thermal conductance of the thermal strap on the TEC performance was discussed previously. The higher the thermal conductance of the thermal strap, the more control power savings can be realized when the TEC is heating the CC, as shown in Figures 14 and 15. Without the thermal strap, the TEC simply degenerates to a regular electrical heater when heating the CC, and no power savings is realized. Without the thermal strap, however, the TEC cannot work as a cooler for the CC because the heat delivered to the hot side of the TEC has nowhere to go. Consequently, a large  $\Delta T$  will build up and the TEC will eventually lose its cooling capability. The TEC may also cease to function as a cooler if the thermal strap has too low a thermal conductance. This can be explained as follows. Because the TEC is directly mounted to the CC, this side of the TEC is at nearly the same temperature as the CC. Because the evaporator is already at a higher temperature than the CC, the TEC hot side must be at an even higher temperature than the evaporator. The smaller the strap thermal conductance, the warmer the TEC hot side will become. Because the cold side temperature is more or less constant (near the CC temperature), a warmer hot side increases the  $\Delta T$  across the TEC, and makes the TEC work less efficiently. More power must be applied to the TEC in order to pump the same amount of heat from the CC. More power to the TEC makes the TEC hot side even warmer and further reduces the effectiveness of the TEC. Thus, a vicious cycle may develop and eventually lead to a total loss of the TEC cooling capability, i.e. the TEC will operate along the 0W heat load line shown in Fig. 5.

There is always a heat leak due to thermal back conduction from the hot side of the TEC to the cold side through the semiconductor p/N pellets, which are needed to carry the electric current. Any heat leak through the P/N pellets adds to the heat load of the TEC, and is included in the TEC performance curves provided by the vendor such as the one shown in Fig. 5. Additional heat leak will also come from the TEC assembly made to satisfy other requirements such as surviving the launch environment. Such heat leak could have important effects to the TEC

performance and should not be overlooked. For the MLHP proto-flight unit, a flexible thermal strap was used to reduce the shear stress imposed on the TEC during launch and a TEC assembly was made to hold to TEC and attach it to the CC as shown in Fig. 22. The TEC was placed inside the bottom copper saddle which was attached to the CC. The TEC was secured by a top copper plate that was connected to the bottom saddle by four stainless steel bolts. To reduce the heat leak from the top plate to the bottom saddle, G10 spacers were used between each bolt and the top plate and between the top plate and the bottom saddle. The top plate was connected to the flexible copper strap. The other end of the strap was connected to another copper saddle attached to the evaporator. To enhance the interfacial thermal conductance, Nusil thermal filler was used on both TEC surfaces. For redundancy, two sets of TEC assemblies were used for each pair of the evaporator and CC. This TEC assembly design was tested in the thermal vacuum chamber. As shown in Fig. 23, four sets of TEC assemblies were installed on the MLHP proto-flight unit, two for each evaporator/CC pair.

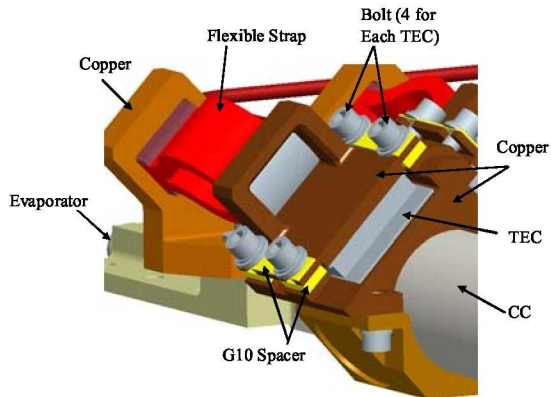


**Figure 22. TEC Assembly for MLHP Proto-flight Unit**

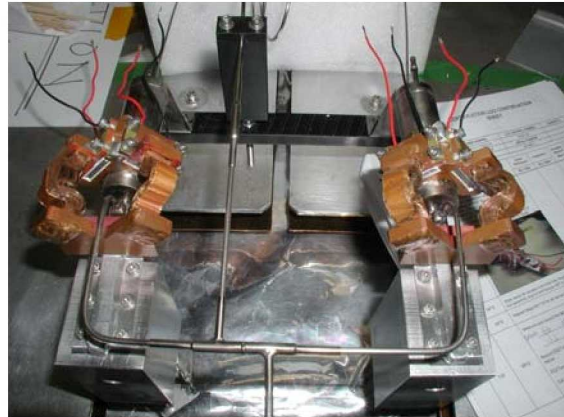


**Figure 23. Picture of TEC Assemblies**

It was found during thermal vacuum testing that the back conductance from the hot side of the TEC to the cold side was higher than calculated. The excessive heat leak was manifested in the CC set point change test where the CC set point temperature was lowered from 303K to 273K with 5K increments. As shown in Fig. 24, the TECs were able to lower the CC temperature with 5K increments from 303K to 288K without any problem. In the next step of lowering the CC temperature to 283K, the CC reached 283K briefly and then rose to 284K and stayed there. Both TECs showed that they drew full power from the power supplies. The reason is that the power applied to the TEC plus the heat leak through the TEC itself and the assembly canceled out the heat being pumped from the CC, and hence no net heat was taken out of the CC. This test was repeated and yielded the same results. Attempt was then made to lower the CC set point with 1K increments. Under this condition, the required TEC voltage and current (power) were reduced, and the TEC was able to lower the CC temperature all the way to 273K as shown in Fig. 24.

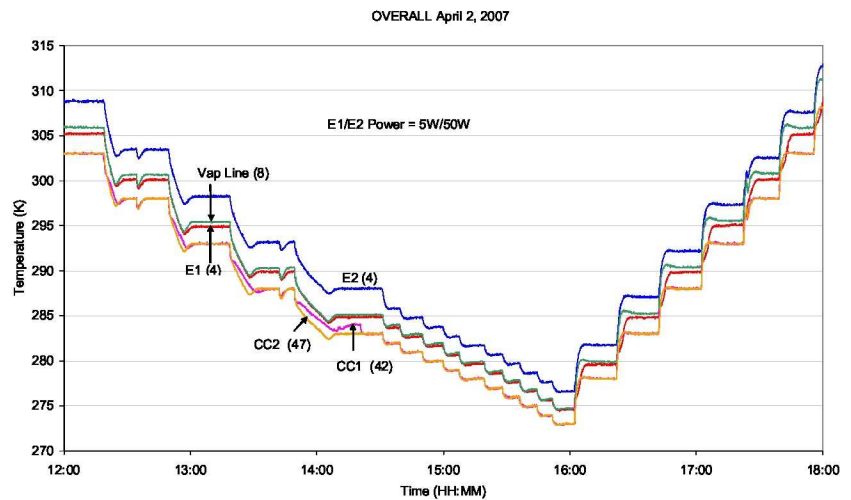


**Figure 24. CC Set Point Change from 303K to 273K**



The TECs were subsequently removed from the MLHP proto-flight unit for examination, and it was found that the Nusil filler spilled into the sides of the bottom copper saddle when the top plate was bolted to the bottom plate as shown in Fig. 25. The Nusil filler was in contact with the top plate and the bottom saddle and provided additional thermal paths for the heat leak.

After the Nusil filler was cleaned, the TECs were reinstalled, and the same CC set point change test was performed. With a smaller thermal leak through the TEC assemblies, the TECs were able to cool the CC with 5K increments, as illustrated in Fig. 26. Note that in Figures 24 and 26, heating the CC by the TECs with 5K increments was never a problem.

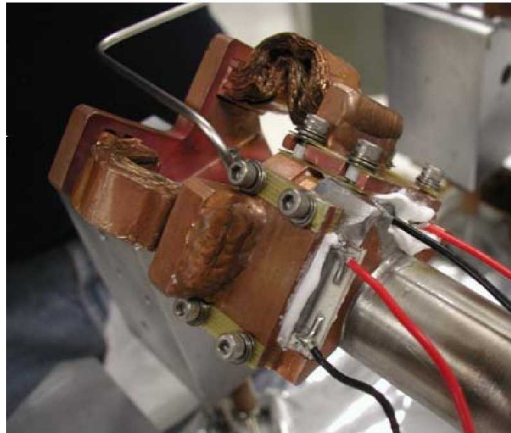


**Figure 25. Spilled Nusil around TEC**

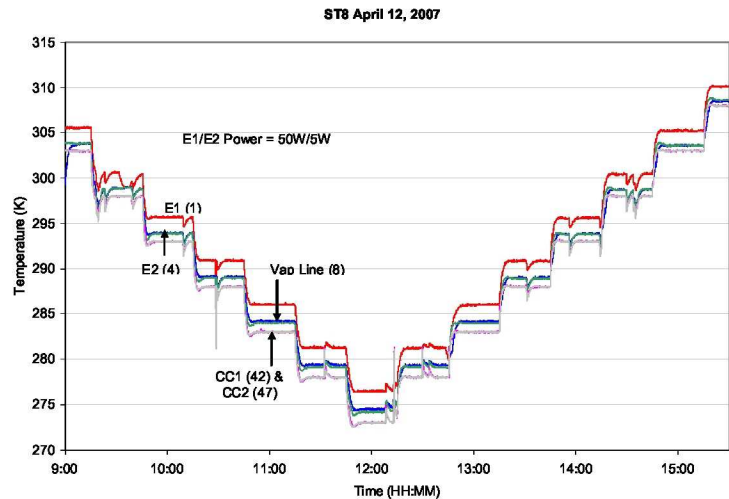


**Figure 26. CC Set Point Change from 303K to 273K**

All TECs have an inherent internal heat leak through the semiconductor P/N pellets. When redundant TECs are used on a CC, an additional heat leak will occur through the idle TEC. For example, the Marlow Model DT3-6 used in this study has a back conduction of about 0.011W/K at 300K. When the active TEC is cooling the CC, its hot side will be warmer than the evaporator. However, the hot side of the idle TEC will be cooler than the evaporator due to the directions of the heat flows, as shown in Fig. 27. This will partially alleviate the adverse effect introduced by the idle TEC. Nevertheless, the additional heat leak must be accounted for in determining the control heater power requirement of the active TEC. When the active TEC is heating the CC, the inactive TEC provides an additional path for heat to flow from the evaporator to the CC, as illustrated in Fig. 28, thereby reducing the control heater power required for the active TEC.

## VI. Summary and Conclusions

A TEC can switch its mode of operation between heating and cooling based on the direction of the electric current flow. A single TEC is therefore capable of providing both heating and cooling to the CC and can be used to control the LHP operating temperature. Several LHPs have used TECs for temperature control in ground tests where one side of the TEC was attached to the CC and the other side was connected to the evaporator through a thermal strap. Using a bi-polar power supply and a control algorithm, the TEC could control the CC temperature within a very tight range through heating and cooling the CC. When heating the CC, the TEC required much less control heater power than the traditional electrical heater. The ability of the TEC to provide cooling to the CC also had additional advantages: 1) The LHP could operate at temperatures below its natural operating temperature at low evaporator heat loads; 2) The LHP could be started successfully even under the worst-case initial condition; and 3) The LHP could be started by simply lowering the CC temperature without applying external power to the evaporator. Tests also verified that the higher the thermal conductance of the thermal strap, the more efficiently the TEC would run.

Because TECs are susceptible to the shear stress, additional measures must be taken in implementing the TEC for space applications. Added features intended to help the TEC withstand the spacecraft launch environment will usually have adverse effects on the TEC thermal performance, and must be taken into consideration. Some lessons learned from past experiences of using TECs include: 1) The TEC is a high current, low voltage device, and the voltage drops along the transmission lines between the power supply and the TEC must be accounted for when applying the current-voltage relation provided by TEC vendors; 2) The thermal back conductance through the TEC



assembly plays an important role in TEC performance, and must be carefully evaluated and experimentally verified;  
 3) When a redundant TEC is used, the back conductance through the inactive TEC must be included in the evaluation of the performance of the active TEC.

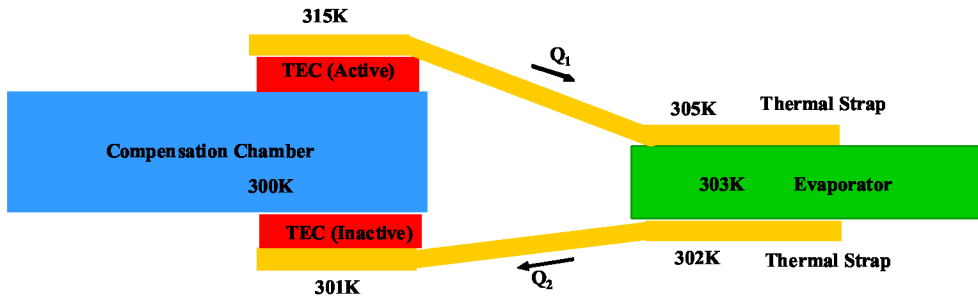


Figure 27. Redundant TECs When CC Is Being Cooled

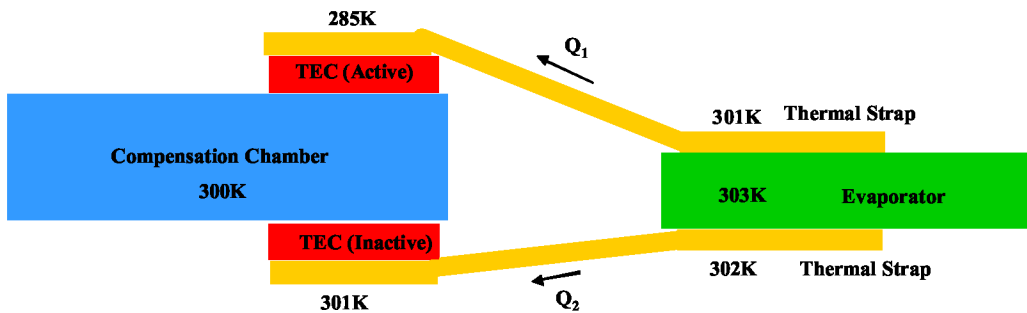


Figure 28. Redundant TECs When CC Is Being Heated

### Acknowledgments

Funding for this investigation was provided by the NASA New Millennium Program. The MLHP Breadboard and proto-flight unit were manufactured by ATK Space Systems in Beltsville, Maryland.

### References

1. Maidanik, Y., and Fershtater, Y., "Theoretical Basis and Classification of Loop Heat Pipes and Capillary Pumped Loops," *10<sup>th</sup> International Heat Pipe Conference, Stuttgart, Germany, 1997*.
2. Ku, J., "Operating Characteristics of Loop Heat Pipes," SAE Paper No. 1999-01-2007, *29<sup>th</sup> International Conference on Environmental Systems, Denver, Colorado, July 12-15, 1999*.
3. Baker, C., Butler, D., Ku, J., and Grob, E., "Acceptance Thermal Vacuum Tests of the GLAS Flight Loop Heat Pipe Systems," *Space Technology and Applications International Forum -2001, Albuquerque, New Mexico, February 11-14, 2001*.
4. Baker, C and Grob, E., "System Accommodation of Propylene Loop Heat Pipes for The Geoscience Laser Altimeter System (GLAS) Instrument," SAE Paper No. 2001-01-2263, *31<sup>st</sup> International Conference on Environmental Systems, Orlando, Florida, July 9-12, 2001*.
5. Baker, C., Butler, D., Ku, J., and Grob, E., "Acceptance Thermal Vacuum Tests of the GLAS Flight Loop Heat Pipe Systems," *Space Technology and Applications International Forum -2001, Albuquerque, New Mexico, February 11-14, 2001*.
6. Grob, E., "System Accommodation of Propylene Loop Heat Pipes for The Geoscience Laser Altimeter System (GLAS) Instrument," Paper No. 2001-01-2263, *31<sup>st</sup> International Conference on Environmental Systems, Orlando, Florida, July 9-12, 2001*.
7. Grob, E., Baker, C., and McCarthy, T., "Geoscience Laser Altimeter System (GLAS) Loop Heat Pipe: An Eventful first Year On-Orbit", Paper No. 2004-01-2558, *34<sup>th</sup> International Conference on Environmental Systems, Colorado Springs, Colorado, July 19-22, 2004*.
8. Ottenstein, L., Ku, J., and Feenan, D., "Thermal Vacuum Testing of a Novel Loop Heat Pipe Design for the Swift BAT Instrument," *Space Technology and Applications International Forum -2003, Albuquerque, New Mexico, February 2-6, 2003*.

9. Choi, M., "Swift BAT Loop Heat Pipe Thermal System Characteristics and Ground/Flight Operation Procedure," Paper No. AIAA 2003-6077, *1<sup>st</sup> International Energy Conversion Engineering Conference, Portsmouth, Virginia, August 17-21, 2003*.
10. Choi, M., "Thermal Vacuum/Balance Test Results of Swift BAT with Loop Heat Pipe Thermal System", AIAA Paper No. 2004-5683, *2<sup>nd</sup> International Energy Conversion Engineering Conference, Providence, Rhode Island, August 16-19, 2004*.
11. Choi, M., "Thermal Assessment of Swift BAT Instrument Thermal Control System In Flight", Paper No. 2005-01-3037, *35<sup>th</sup> International Conference on Environmental Systems, Rome, Italy, July 11-14, 2005*.
12. Goncharov, K., "Development of Loop Heat Pipe with Pressure Regulator," Paper No. 2006-01-2171, *36<sup>th</sup> International Conference on Environmental Systems, Norfolk, Virginia, July 17-20, 2006*.
13. Goncharov, K. and Kolesnikov, V., "Development of Propylene Loop Heat Pipe for Spacecraft Thermal Control", in Proc. of *12<sup>th</sup> International Heat Pipe Conference, Moscow, Russia, May 19-24, 2002*, pp. 171-176.
14. Bodendieck, F., Schlitt, R., Romberg, O., Goncharov, K., Buz, V. and Hildebrand, U., "Precision Temperature Control with a Loop Heat Pipe", Paper No. 2005-01-2938, *35<sup>th</sup> International Conference on Environmental Systems, Rome, Italy, July 11-14, 2005*.
15. Grinier, H., Feuillatre, M., Maciaszek, T., and Hustaix, H., "Development and Test Results of a 5kW Ammonia Capillary Pumped Loop," Paper No. 951505, *25<sup>th</sup> International Conference on Environmental Systems, San Diego, California, July 10-13, 1995*.
16. Rodriguez, J. I., Na-Nakompanom, A., Rivera, J., Mireles, V. and Tseng, H., "On-Orbit Thermal Performance of the TES Instrument – Three Years in Space," SAE Paper No. 2008-01-2118, *38<sup>th</sup> International Conference on Environmental Systems, San Francisco, California June 30 - July 2, 2008*.
17. Nikitkin, M. and Wolf, D., "Development of LHP with Low Control Power," Paper No. 2007-01-3237, *37<sup>th</sup> International Conference on Environmental Systems, Chicago, Illinois, July 9-12, 2007*.
18. Nikitkin, M. N., Kotlyarov, E. Y. and Serov, G. P., "Basics of Loop Heat Pipe Temperature Control", Paper No. 1999-01-2012, *29<sup>th</sup> International Conference on Environmental Systems, Denver, Colorado, July 12-15, 1999*.
19. Ku, J., "Methods of Controlling the Loop Heat Pipe Operating Temperature," SAE Paper No. 2008-01-1998, *38<sup>th</sup> International Conference on Environmental Systems, San Francisco, California, June 30 - July 2, 2008*.
20. Rowe, D. M., (ed.), *CRC handbook of Thermoelectrics*, CRC Press,, New York, 1995.
21. Ku, J., Jeong, S., and Butler, D., "Testing of a Miniature Loop Heat Pipe with Thermal Electrical Cooler for Temperature Control," SAE Paper No. 2004-01-2505, *34<sup>th</sup> International Conference on Environmental Systems, Colorado Springs, Colorado, July 19-22, 2004*.
22. Ku, J., Ottenstein, L., and Birur, G., "Thermal Performance of a Multi-Evaporator Loop Heat Pipe with Thermal Masses and Thermoelectric Coolers", *13<sup>th</sup> International Heat Pipe Conference, Shanghai, China, September 21-25, 2004*.
23. Ku, J. and Nagano, H., "Using Thermoelectric Converters for Loop Heat Pipe Operating Temperature Control," AIAA Paper No. AIAA-2006-4057, *4<sup>th</sup> Intersociety Energy Conversion Engineering Conference, San Diego, California, June 26-29, 2006*.
24. Ku, J. and Nagano, H., "Loop Heat Pipe Operation with Thermoelectric Converters and Coupling Blocks," AIAA Paper No. AIAA-2007-4713, *5<sup>th</sup> Intersociety Energy Conversion Engineering Conference, St. Louis, Missouri, June 25-27, 2007*.
25. Ku, J., Ottenstein, L., Butler, D. and Nagano, H., "Thermal Performance of a Miniature Loop Heat Pipe with Multiple Evaporators and Multiple Condensers," *14<sup>th</sup> International Heat Pipe Conference, Florianópolis, Brazil, April 22-27, 2007*.
26. Ku, J., Ottenstein, L., and Nagano, H., "Thermal Vacuum Testing of a Miniature Loop Heat Pipe with Multiple Evaporators and Multiple Condensers," Paper No. HT2007-32302, *2007 ASME/JSME Thermal Engineering Summer Heat Transfer Conference, Vancouver, British Columbia, Canada, July 8-12, 2007*.
27. Ku, J., Ottenstein, L., Douglas, D., and Hoang, T., "Multi-Evaporator Miniature Loop Heat Pipe for Small Spacecraft Thermal Control, Part 1: New Technologies and Validation Approach," AIAA Paper No. 2010-1493, *48<sup>th</sup> AIAA Aerospace Science Meeting, Orlando, Florida, January 4-7, 2010*.
28. Ku, J., Ottenstein, L., Douglas, D., and Hoang, T., "Multi-Evaporator Miniature Loop Heat Pipe for Small Spacecraft Thermal Control, Part 2: Validation Results," AIAA Paper No. 2010-1494, *48<sup>th</sup> AIAA Aerospace Science Meeting, Orlando, Florida, January 4-7, 2010*.
29. Maidanik, Y. F., Solodovnik, N. N., and Fershtater, Y. G., "Investigation of Dynamic and Stationary Characteristics of a Loop Heat Pipe," *IX International Heat Pipe Conference, Albuquerque, New Mexico, May 1-5, 1995*.
30. Ku, J. and Nagano, H., "Effects of Gravity on Start-up and Heat Load Sharing of a Miniature Loop Heat Pipe," SAE Paper No. 2007-01-3234, *37<sup>th</sup> International Conference on Environmental Systems, Chicago, Illinois, July 9-12, 2007*.